

# A credit-card library approach for disrupting protein–protein interactions

Yang Xu,<sup>a</sup> Jin Shi,<sup>b</sup> Noboru Yamamoto,<sup>a</sup> Jason A. Moss,<sup>a</sup>  
Peter K. Vogt<sup>b,\*</sup> and Kim D. Janda<sup>a,\*</sup>

<sup>a</sup>*Department of Chemistry and Immunology, The Skaggs Institute for Chemical Biology and Worm Institute for Research and Medicine (WIRM), The Scripps Research Institute, 10550 North Torrey Pines Road, La Jolla CA 92037, USA*

<sup>b</sup>*Department of Molecular and Experimental Medicine, The Scripps Research Institute, 10550 North Torrey Pines Road, La Jolla, CA 92037, USA*

Received 23 November 2005; accepted 23 November 2005

Available online 27 December 2005

**Abstract**—Protein–protein interfaces are prominent in many therapeutically important targets. Using small organic molecules to disrupt protein–protein interactions is a current challenge in chemical biology. An important example of protein–protein interactions is provided by the Myc protein, which is frequently deregulated in human cancers. Myc belongs to the family of basic helix–loop–helix leucine zipper (bHLH-ZIP) transcription factors. It is biologically active only as heterodimer with the bHLH-ZIP protein Max. Herein, we report a new strategy for the disruption of protein–protein interactions that has been corroborated through the design and synthesis of a small parallel library composed of ‘credit-card’ compounds. These compounds are derived from a planar, aromatic scaffold and functionalized with four points of diversity. From a 285 membered library, several hits were obtained that disrupted the c-Myc–Max interaction and cellular functions of c-Myc. The IC<sub>50</sub> values determined for this small focused library for the disruption of Myc–Max dimerization are quite potent, especially since small molecule antagonists of protein–protein interactions are notoriously difficult to find. Furthermore, several of the compounds were active at the cellular level as shown by their biological effects on Myc action in chicken embryo fibroblast assays. In light of our findings, this approach is considered a valuable addition to the armamentarium of new molecules being developed to interact with protein–protein interfaces. Finally, this strategy for disrupting protein–protein interactions should prove applicable to other families of proteins.  
© 2005 Elsevier Ltd. All rights reserved.

## 1. Introduction

The biological function of a protein is often determined by its interactions with other protein molecules.<sup>1–4</sup> Because of the critical role of such protein–protein interactions in many cellular processes, the development of modulators able to interfere with specific interactions has emerged as an important goal. Ultimately, specific control of protein functions may offer therapeutic benefits. Cell-permeable small organic molecules are of particular interest as modulators of protein–protein interactions, but the discovery of effective compounds is challenging.<sup>5–7</sup> Chemical entities that have been designed to interact with specific binding motifs often

do not target a specific protein–protein interaction, probably because of the complexity of the recognition mechanism.<sup>8,9</sup> To address such issues, the use of combinatorial chemical libraries containing small organic molecules holds promise as a powerful approach in the identification of novel lead compounds.<sup>7,10–15</sup>

Myc and its partner protein Max belong to the basic helix–loop–helix leucine zipper (bHLH-LZ) protein family.<sup>16–23</sup> Myc is a transcription factor with oncogenic and apoptotic potential.<sup>24–26</sup> The role of Myc in tumorigenesis has been linked to its transcriptional activities, promoting cell growth and repressing differentiation. Myc shows gain of function in numerous and diverse human cancers including Burkitt’s lymphoma, neuroblastoma, lung, breast, and colon carcinomas. The oncogenic activity of Myc depends on dimerization with Max via the helix–loop helix and leucine zipper domains.<sup>27–30</sup> Myc cannot form homodimers, and in order to bind to its DNA target sequence, the E box

*Keywords:* Credit-card library; Myc–Max; Protein–protein interactions; Oncogenic transformation; Transcriptional regulation.

\* Corresponding authors. Tel.: +1 858 784 2516; fax: +1 858 784 2595; e-mail: [kdjanda@scripps.edu](mailto:kdjanda@scripps.edu)

element (CACGTG), Myc must associate with Max. The inhibition of Myc–Max dimerization is an enticing drug target, since inhibitors may prevent tumorigenesis and, more generally, could serve as a proof-of-principle for the design of small molecule inhibitors of protein–protein interactions.

The structural stability of protein–protein interactions derives from large (typically 1000–3000 Å<sup>2</sup>), but relatively shallow, interfaces.<sup>31–34</sup> The difficulty of disrupting such expansive interactions with small molecules has been linked to the area of the more buried surfaces. Breakthroughs in breaching such interactions have occurred with the identification of ‘hot spots’.<sup>35,36</sup> These domains have been characterized as shallow loci of about 600 Å<sup>2</sup> found at, or near, the geometric center of the protein–protein interface, and certain amino acids in hot spot regions contribute significantly to the stability of the protein–protein complexes. These amino acids are usually aromatic, such as tryptophan, tyrosine, and histidine, along with other hydrophobic residues.<sup>37,38</sup>

In considering structural information, modeling analysis, and the recent identification of peptidomimetic and small molecule inhibitors of protein–protein interactions, we designed a new scaffold aimed at hot spot specificity and, hence, the disruption of protein–protein interactions. We viewed hot spots at interfaces between proteins as aromatic, slot-like regions or ‘card readers’ characteristically different from the deeper binding clefts often found within proteins. Logically, insertion of a ‘credit-card’ into the locale of the reading interface should trigger an event at the interface. This conceptual approach led to what we term ‘credit-card’ compounds upon which to base a small molecule library.

As the name implies, the credit-card library members are simply planar, aromatic core structures elaborated with chemical diversity. However, while this notion is rather simplistic, we note that our overall structural design of this library should provide favorable enthalpic contributions from van der Waals interactions,  $\pi$ -stacking, possible desolvation, and favorable entropy gains from hydrophobic effects. In total, the compounds are intended to function as inhibitors of protein–protein interactions or otherwise alter/disrupt the necessary

communication at the interface. Herein, we report the design and parallel synthesis of a credit-card library. Furthermore, we show the usefulness of the library for the discovery of small molecule inhibitors of Myc–Max dimerization and, importantly, the biological effect of these inhibitors on Myc activity in chicken embryo fibroblast assays.

## 2. Results

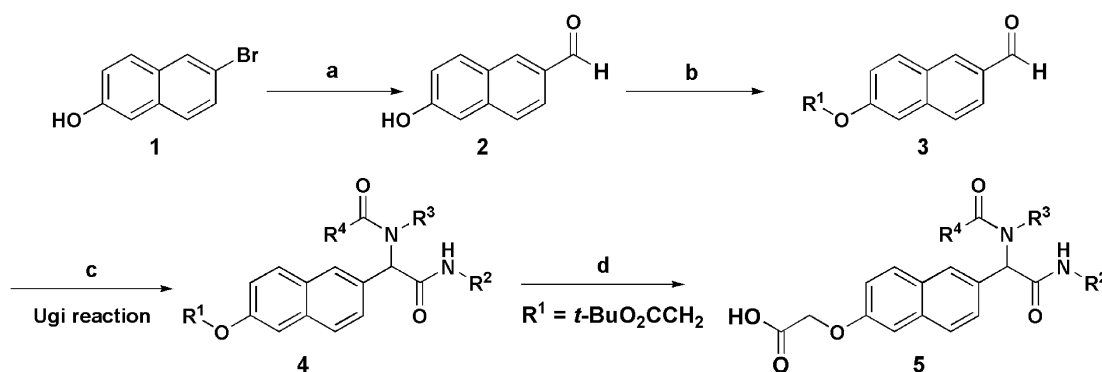
### 2.1. Library design

To design and generate the library, we chose a multiple-component reaction, namely the Ugi reaction.<sup>39–42</sup> Multiple-component reactions use three or more reactants in a one-pot procedure to form a product that contains structural aspects of each of the components.<sup>43</sup> The reactions are versatile and can be carried out in solution or on a solid support in parallel fashion. For the Ugi reaction, we employed a naphthalene-based template<sup>44</sup> as a rigid, planar, aromatic core (Scheme 1) and a set of components that would introduce additional diversity (Fig. 1).

Hence, appended  $\alpha$ -acylamino amide diversity would be attached to the naphthyl scaffold **2** to generate general structure **5** (Scheme 1). Parallel solution-phase methodology was employed to generate the library because of its medium size, non-limiting scale, and ease of resynthesis of hits in a short period of time.<sup>7,11,45</sup> The general building blocks for this library in total would allow an extended structure into both two- and three-dimensional space. To initially explore structure–activity relationships surrounding the planar template, we functionalized the naphthalene core with motifs that spanned a wide range of size, polarity, aromaticity, and hydrogen-bonding capability. Our hope was that a high degree of diversity in scaffold functionalization would allow a thorough investigation of the chemical basis for small molecule inhibition of protein–protein interactions.

### 2.2. Library preparation

A two- or three-step synthesis was used as our general procedure (Scheme 1). The key component to our credit-



**Scheme 1.** General synthetic design of the ‘credit-card’ library. Reagents and conditions: (a) *n*-BuLi (2 equiv), THF, –78 °C, then DMF; (b) R<sup>1</sup>Br, K<sub>2</sub>CO<sub>3</sub>, DMF, 60 °C; (c) R<sup>2</sup>NC, R<sup>3</sup>NH<sub>2</sub>, R<sup>4</sup>CO<sub>2</sub>H, MeOH (and CHCl<sub>3</sub>), reflux; (d) TFA, CH<sub>2</sub>Cl<sub>2</sub>, 0 °C.

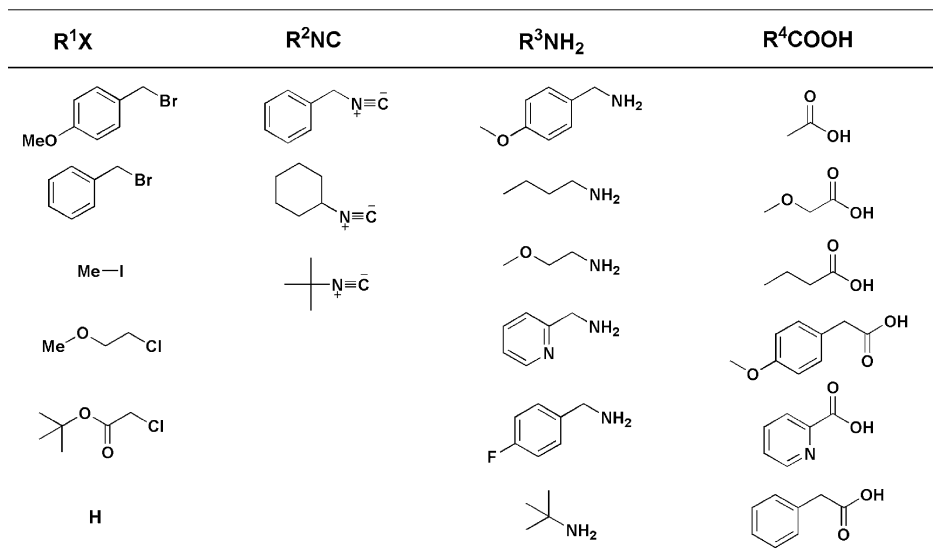


Figure 1. Components utilized in the library preparation.

card design was 6-hydroxy-naphthalene-2-carbaldehyde **2** that was obtained from commercially available 6-bromo-2-naphthol **1**, using *n*-BuLi and DMF as an electrophilic trapping agent (Scheme 1). Treatment of **2** with a variety of halides (R<sup>1</sup>X) provided **3** in good to moderate yields under basic conditions. The Ugi reaction and our library synthesis were conducted using a combination of isocyanides (R<sup>2</sup>NC), amines (R<sup>3</sup>NH<sub>2</sub>), and carboxylic acids (R<sup>4</sup>CO<sub>2</sub>H) with naphthol derivatives **2** or **3**. As anticipated, the Ugi reactions proceeded well, and in virtually all cases the desired multi-component products eluted between by-products and starting materials on silica gel. Hence, products were easily purified by short column chromatography using 2 mL of silica gel in a 5 mL polypropylene fritted syringe, upon eluting with 10–50% of EtOAc/hexane. When R<sup>1</sup> was the acetic acid *tert*-butyl ester, the product **4** was treated with TFA to provide acid derivatives **5**. Finally, all library members were characterized by <sup>1</sup>H NMR and produced in high purities (greater than 95%) with yields ranging from 30% to 99% on a multi-milligram scale (typically 20–100 mg).

### 2.3. Screening for inhibitors of Myc–Max dimerization

Initial screening for compounds that interfere with the Myc–Max interaction was carried out by fluorescence resonance energy transfer (FRET) using the 96-well microplate platform and following previously described methods.<sup>11</sup> Briefly, the basic helix–loop–helix leucine zipper domains of Myc and of Max, linked to a cyan fluorescent protein and yellow fluorescent protein, respectively, were produced in bacteria and purified on Ni columns using a His-Tag motif incorporated in the constructs. Interaction of the purified proteins produced a strong FRET signal characterized by an emission peak at 525 nm. All compounds from the library were examined at 7.6 μM. A reduction in fluorescence at 525 nm by 25% was considered a positive hit and was selected for further study. From the library of 285 credit card-like

compounds, 40 were selected. These 40 compounds were studied in greater detail by electrophoretic mobility shift assay (EMSA). Four representative examples are shown in Figure 2.

DNA-binding by Myc requires dimerization with Max, and inhibitors of dimerization are ipso facto inhibitors of DNA-binding. EMSA was performed following published techniques.<sup>11</sup> The target oligonucleotide with the consensus binding site of Myc–Max dimers was 5'AGTTGACCACGTGGTCTGGG3'. It was labeled with γ-<sup>32</sup>P-ATP by T4 polynucleotide kinase. The basic helix–loop–helix leucine zipper domains of Myc (50 nM) and of Max (27.5 nM), purified from Ni columns, were first allowed to dimerize in the presence or absence of various amounts of the compound for 1 h at room temperature and were then incubated with the target oligonucleotide at a concentration of 60 pg/μL (50,000 cpm) for 30 min. Protein–DNA complexes were resolved on 4% acrylamide gels and detected by autoradiography. From the four representative compounds shown in Figure 3, dose–response curves using EMSA were determined and yielded IC<sub>50</sub> values from 17 to 36 μM (Fig. 4 and Table 1).

The four selected compounds were reexamined in single-cuvette FRET assays to confirm the EMSA results and at 7.6 μM inhibited dimerization to extents of between 66% (NY2276) and 36% (NY2280) (data not shown). In contrast, three control compounds representing the core scaffolds **6–8** (Fig. 5) failed to inhibit the Myc–Max FRET signal.

### 2.4. Biophysical analysis for putative denaturation of Myc–Max complex by selected library members

To confirm that selected compounds disrupted the Myc–Max complexation by a mechanism other than non-specific denaturation, a synthetic Myc–Max dimer was prepared by chemical synthesis; its helicity was then

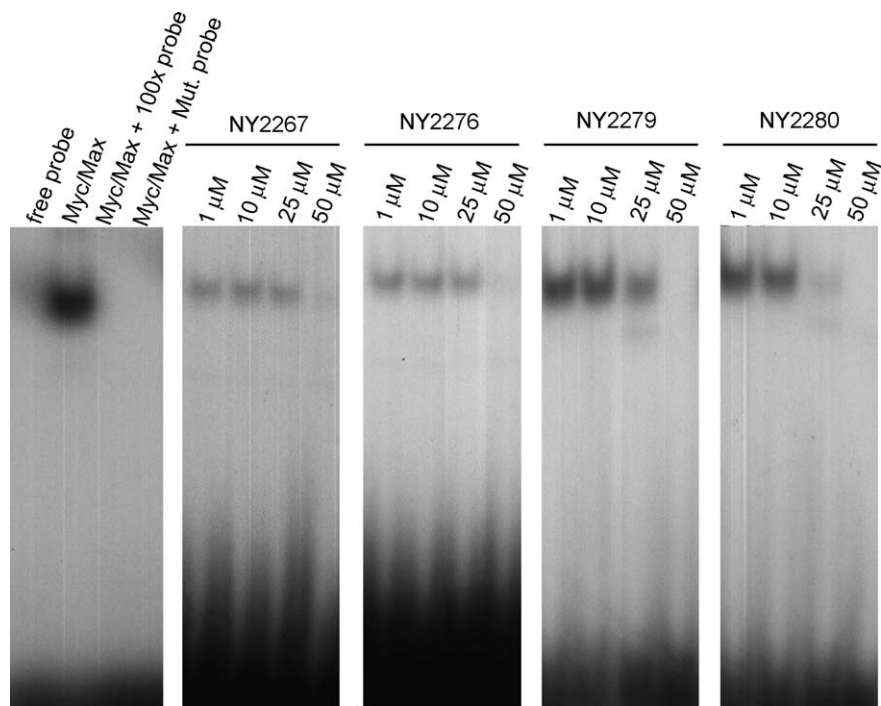


**Figure 2.** Inhibition of Myc–Max DNA-binding as determined by EMSA. Left panel: control reactions showing the mobility shift induced by Myc–Max, inhibition of the shift by a 100-fold excess of unlabeled probe, and failure of Myc–Max to bind to a mutated probe (5'AGTTGACTACGTAGTCTGGG3'). The four panels to the right depict EMSA inhibition achieved at various concentrations of four selected compounds (see Fig. 3) from the 285-membered library.

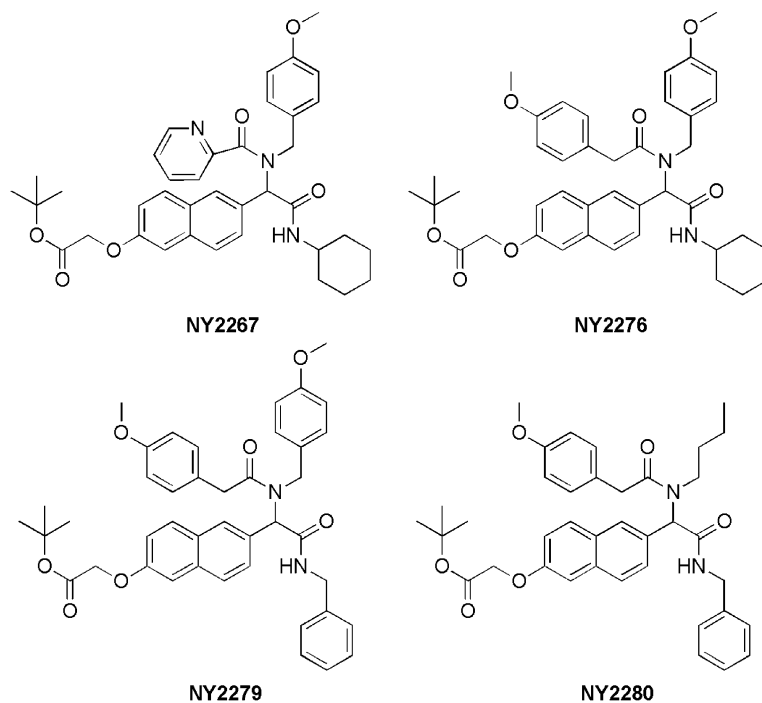


**Figure 3.** Selected compounds from EMSA.

studied by far-UV circular dichroism in the presence and absence of the selected compounds. For this purpose, a covalent, 'tethered' Myc–Max dimer was prepared using thioether ligation chemistry from separately synthesized Myc and Max peptides bearing mutually reactive func-

tionality. This chemistry was chosen because it can be performed chemoselectively in the context of all other functionalities in the Myc and Max peptides in aqueous solution allowing for high solubility and facile monitoring by reversed-phase (RP) HPLC. Hodges and

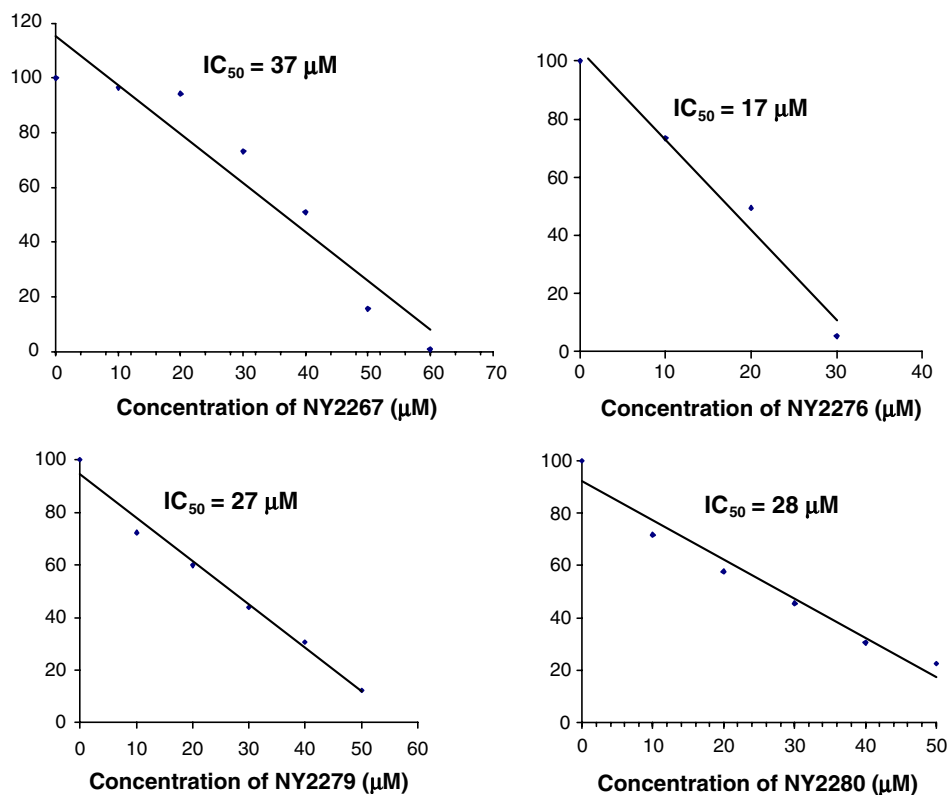


**Figure 4.** Dose–response determination by EMSA. EMSA was performed with serial dilutions of each compound and the degree of inhibition was measured by densitometry of the shifted band. Densitometry was carried out by using the NIH Image 1.63 software program.  $IC_{50}$  values were determined arithmetically from the slopes of the dose–response curves.

**Table 1.**  $IC_{50}$  values determined for the four compounds selected by EMSA

Compound	$IC_{50}$ ( $\mu M$ ) <sup>a</sup>
NY2267	36.5
NY2276	17.3
NY2279	26.9
NY2280	28.1

<sup>a</sup> DNA-binding EMSA was performed with serial dilutions of each compound and the degree of inhibition determined by densitometry of the shifted band. Densitometry was performed using NIH Image 1.63 software program.

co-workers<sup>46,47</sup> have prepared a covalent, tethered Myc–Max dimer using a disulfide linkage and verified the resulting conjugate’s helicity. However, whereas the formation of mixed homo- and heterodimers is often problematic in the case of disulfide linkage chemistry, thioether ligation is performed under reducing conditions, thereby affording the desired compound in near-quantitative yield.

The final step in the synthesis of the covalent Myc–S–Max conjugate is shown in Figure 6. BrAc–Myc and

Mpa–Max were prepared by automated, stepwise solid-phase peptide synthesis (SPPS) using custom-modified in situ neutralization protocols for Boc chemistry. Both peptides were easily solubilized to 10 mg/mL in  $N_2$ -purged 0.5 M triethanolamine, pH 8.0, containing 6 M guanidine hydrochloride. After 16 h reaction at ambient temperature, RP-HPLC/MS analysis indicated that this reaction was complete, and the product was purified by preparative RP-HPLC (Fig. 7). It should be noted that the product elutes only 0.2 min later than the unreacted Mpa–Max peptide, which is commensurate with previous work<sup>46,47</sup> MS analysis was critical in confirming the absence of any contaminating unreacted material in the full-length product.

The purified, lyophilized Myc–S–Max construct was then reconstituted in phosphate-buffered saline (PBS), pH 7.4, at 100  $\mu M$ . This solution was then diluted 10-fold into separately prepared 25  $\mu M$  solutions of NY2267, NY2276, NY2279, and NY2280 in PBS containing 5 vol % DMSO. After 14 h equilibration, these four solutions were subjected to far-UV circular dichroism analysis and compared with a solution of

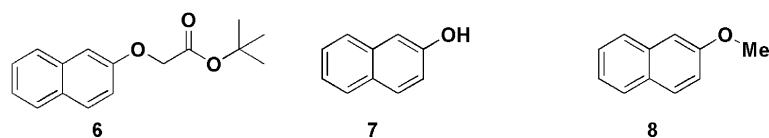


**Figure 5.** Control compounds, 6–8, used in the FRET, EMSA, and transcriptional regulation assays.

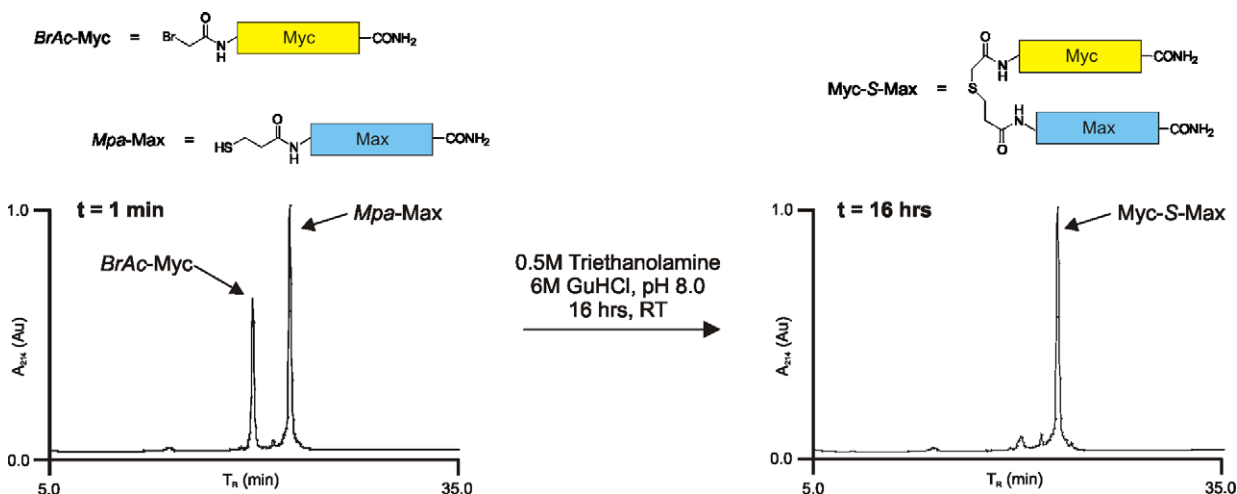


Figure 6. Synthesis of the Myc-S-Max construct by thioether ligation.

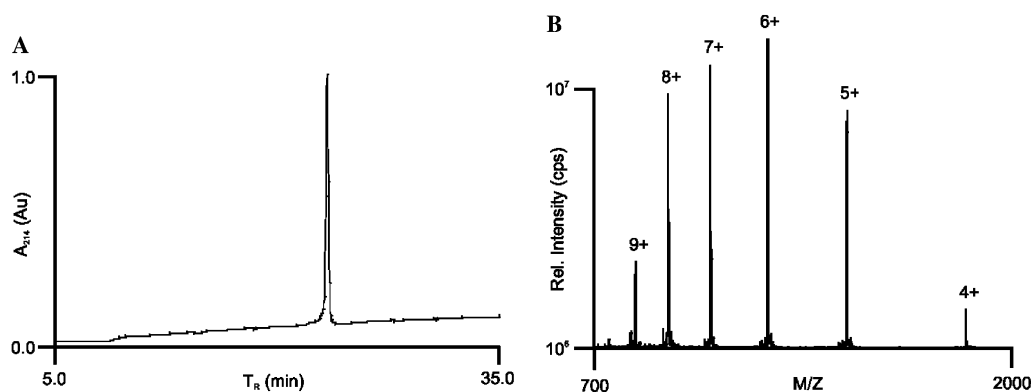


Figure 7. (A) Analytical RP-HPLC and (B) raw ESI-MS data for the purified Myc-S-Max construct.  $M/Z$  ion charge states are accurate to  $\pm 0.05\%$  of theory (see Section 5).

Myc-S-Max only. After overnight incubation, no gross change in the helicity of the Myc-S-Max construct was observed (Fig. 8), both with regard to intensity and the wavelength of global and local minima (208 and 221 nm, respectively). This implies that at their  $IC_{50}$  concentration, these compounds do not exert their effects on the Myc-Max dimer by a denaturation-type mechanism. However, this CD experiment can not clarify if in the presence of the four selected compounds, at their  $IC_{50}$  concentrations, the Myc-S-Max construct still exists as a ‘tethered’ dimer. In total, these compounds may disrupt the inter-helix contacts between the Myc and Max sequences, thereby yielding a similar per-residue normalized helicity signal while being spatially separated from one another.

### 2.5. Effect of NY2267, NY2276, NY2279, and NY2280 on oncogenic transformation

The four selected compounds inhibiting the Myc-Max interactions in EMSA and FRET assays were investigated for their effects on oncogenic transformation induced by retroviruses in chicken embryo fibroblasts (CEF).

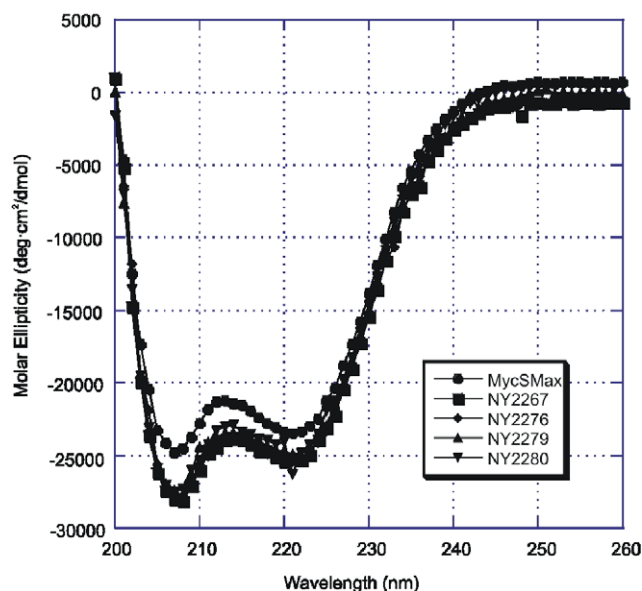


Figure 8. Circular dichroism study of the synthetic Myc-S-Max construct, alone and in the presence of the four NY compounds.

CEF were infected with viruses expressing the Myc, Jun, P3K, and Src oncoproteins, and were then treated for the duration of the experiment with 20  $\mu$ M of the NY and control compounds. Transformed cell foci were counted after three weeks, and the efficiencies of transformation were determined for the oncoprotein–compound combinations (Table 2). In viewing Table 2, the following conclusions can be made: (1) **NY2267** and **NY2280** (see Fig. 9) strongly inhibited oncogenic transformation induced by Myc; (2) **NY2276** and **NY2279** were not effective in transformation assays, although **NY2276** caused some cytotoxicity that varied in extent with different avian embryos and appeared to affect preferentially Myc-transformed cells; (3) **NY2280** had a modest inhibitory effect on focus formation by Jun (Fig. 9); (4) three of the four compounds reduced focus counts in cultures infected with P3K-expressing virus, but similar reductions were seen with a control compound, and we view this mild effect as non-specific.

**Table 2.** Efficiency of oncogenic transformation induced by various oncoproteins in the presence of selected library compounds and controls

Compound	Oncoprotein			
	Myc	Src	Jun	P3K
<b>NY2267</b>	0.05 $\pm$ 0.01	0.85 $\pm$ 0.03	1.02 $\pm$ 0.28	0.38 $\pm$ 0.05
<b>NY2279</b>	0.41 $\pm$ 0.01	0.92 $\pm$ 0.01	1.05 $\pm$ 0.30	0.31 $\pm$ 0.05
<b>NY2276</b>	1.07 $\pm$ 0.01	ND	0.42 $\pm$ 0.01	0.95 $\pm$ 0.20
<b>NY2280</b>	0.06 $\pm$ 0.01	0.80 $\pm$ 0.03	0.28 $\pm$ 0.05	0.32 $\pm$ 0.03
<b>7</b>	1.06 $\pm$ 0.02	1.24 $\pm$ 0.32	ND	1.37 $\pm$ 0.63
<b>8</b>	0.62 $\pm$ 0.02	1.27 $\pm$ 0.35	ND	0.40 $\pm$ 0.25

Efficiency of transformation is defined as the focus forming titer of the oncoprotein expression vector in the presence of compound over the titer in the absence of compound. Strong inhibition of Myc-induced oncogenicity is indicated by bold numbers. ND = not determined.

## 2.6. Effect of NY2267, NY2276, NY2279, NY2280 and simple core scaffolds 6–8 on transcriptional regulation

We tested **NY2267**, **NY2276**, **NY2279**, **NY2280** and three negative controls, 6–8, for their ability to affect rates of transcription in reporter assays. Cells were transfected with an expression construct of a transcriptional activator (Myc, Jun, or NFkB) and with a luciferase reporter construct whose expression is activated by the transfected activator. The luciferase values obtained for an activator–reporter combination in the absence of an experimental compound were set as 1.00. Luciferase values obtained in the presence of test compounds were expressed as fractions of these activator–reporter controls (Table 3). Myc- and Jun-induced transcriptional activation was inhibited by the four NY compounds. There was no significant effect on transactivation by NFkB with any of the compounds. Furthermore, the negative control compounds did not interfere with the transcriptional activation by Myc, Jun or NFkB.

## 3. Discussion

The conceptual and practical approaches toward organic reactions and drug discovery are in the midst of a revolution. The discrete synthesis and biological screening of individual compounds that often takes years to find and optimize leads are being supplanted by emerging technologies. On one hand, structure-based design has entered a new era driven by advances in X-ray instrumentation, automation, and computation with a focus on proteins derived from the genome project. On the other hand, combinatorial chemistry has provided access to a variety of compound libraries in a short period of time, and the technologies are generally more readily available.<sup>48–52</sup> In conjunction with the latter approach,

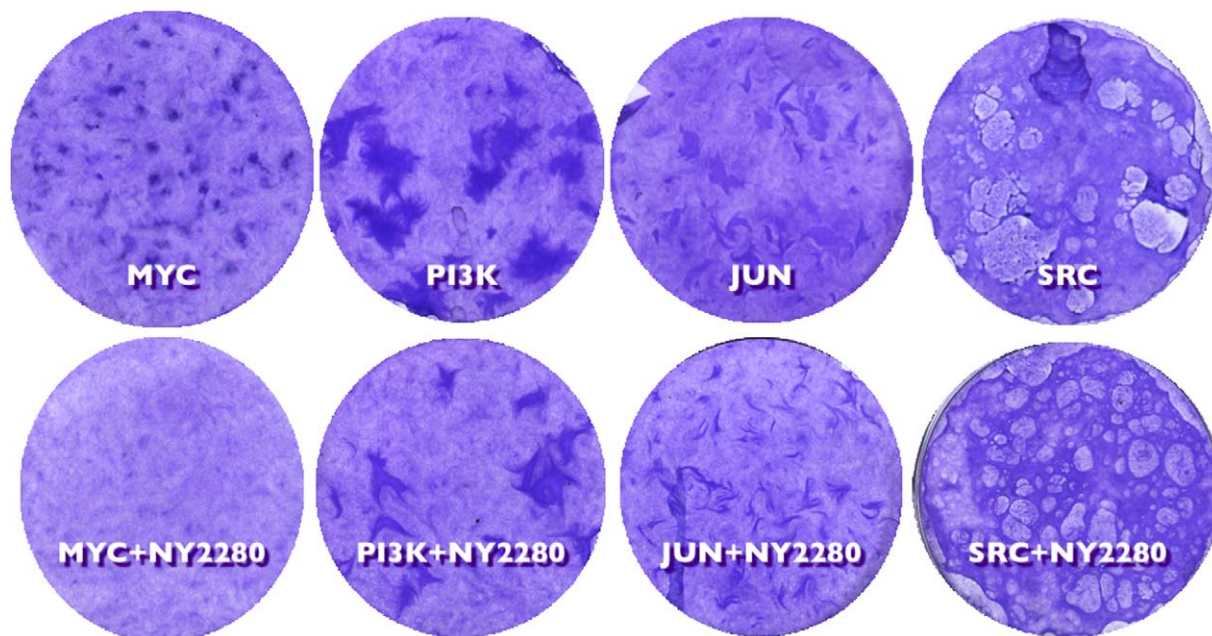


**Figure 9.** Formation of transformed cell foci in monolayer cultures of CEF in the absence or presence of 20  $\mu$ M NY2280.

**Table 3.** Effect of NY and control compounds on transcriptional regulation

Compound	Transcriptional activation		
	Myc <sup>a</sup>	Jun <sup>b</sup>	NFkB <sup>c</sup>
None (vector control)	1.00	1.00	1.00
<b>NY2267</b>	0.38 ± 0.05	0.26 ± 0.01	0.93 ± 0.03
<b>NY2276</b>	0.27 ± 0.03	0.35 ± 0.02	1.02 ± 0.09
<b>NY2279</b>	0.40 ± 0.05	0.35 ± 0.03	1.05 ± 0.09
<b>NY2280</b>	0.51 ± 0.04	0.35 ± 0.04	0.86 ± 0.12
<b>6</b>	1.11 ± 0.10	1.17 ± 0.23	1.51 ± 0.29
<b>7</b>	ND	1.26 ± 0.27	0.78 ± 0.17
<b>8</b>	0.88 ± 0.11	1.21 ± 0.15	1.12 ± 0.15

<sup>a</sup> HEK293 cells were transfected with the pCVMV3HuMyc construct which expresses human Myc from the CMV promoter in a pcDNA3 vector backbone. The reporter construct was pGL2M4, which contains the luciferase gene controlled by four Myc binding sites in the SV40 promoter of the pGL2 vector. Vector control represents transfection of the Myc and reporter vectors without experimental compound; it was arbitrarily set as 1. Standardization was carried out with the Renilla vector pRLCM.

<sup>b</sup> JEG-3 cells were transfected with pHygEF2-c-Jun in which expression of full length c-Jun is controlled by the promoter of elongation factor 1a. The reporter vector used was 3 × 11#pRNGP-luciferase. Vector control represents transfection of the Jun and reporter constructs without experimental compound. Standardization was carried out with the pRLCMV Renilla expression vector.

<sup>c</sup> HEK293 cells were transfected with the CMX-p50 and CMX-p65 constructs expressing NFkB p50 and p65, respectively. The reporter construct was NFkB-Luc containing five NFkB binding sites in the promoter controlling the firefly luciferase gene. Vector control represents transfection of the NFkB and reporter vectors without experimental compound; it was arbitrarily set as 1. Standardization was carried out with Renilla vector pRLCMV.

high-throughput screening methods can rapidly identify lead compounds and yield information for subsequent optimization.<sup>53–56</sup> The development and application of combinatorial chemical libraries derived from split-mix and/or parallel synthesis are now widely utilized in the search for new drugs.

To exploit fully the interplay between proteins discovered from the genome and combinatorial technology, drug design concepts must be evolved by examining alternative ways of thinking. A case in point can be found in the disruption of protein–protein interactions using small synthetic molecules that is currently considered a challenging target for drug discovery.<sup>57–61</sup> One of the most cited difficulties for a synthetic molecule in disrupting protein–protein interactions is that relatively large protein surface areas—on the order of 1000–3000 Å<sup>2</sup> in size and stabilized by multiple interactions—must be ‘out-competed’ by the target molecule. The nature of the binding surface between two proteins may be a more practical concern. These surfaces lack distinct pockets and are largely devoid of discrete binding sites that could accommodate small molecules. The situation is quite distinct from that of mimicking small molecule ligands for enzymes or protein receptors in which the combining sites are most often found at the hydrophobic interior of proteins with little or no aqueous solvation. Within the confines of a highly organized pocket evolved to bind a small substrate, ligand func-

tional groups can efficiently interact with the protein and account for large binding energies.

In spite of the perceived difficulties associated with binding a vast surface area at a protein–protein interface, the binding energy of the interactions within this space is not evenly dispersed. The identification of protein hot spots has provided new insight into the interface domain. As demonstrated by Wells and co-workers, one can generate a comparative map of mutant proteins where mutations that contribute most to the loss of affinity are near each other on the protein surface and that the residues are not necessarily contiguous in the primary sequence of the protein.<sup>62</sup> Surrounding the hydrophobic hot spot are regions of residues that contribute less to the stabilization of the complex. Thus, the ~600 Å<sup>2</sup> area of the hot spot may be the size critical to make a water-excluded seal and promote energetically favorable contributions of hydrogen-bonding and electrostatic interactions. Furthermore, just as solvation of hydrophobic residues can be important in the unfolding of proteins, solvation at the interface could disrupt protein–protein interactions. Hence, rather than dealing with the formidable task of specifically binding the entire protein–protein interface, we chose only to conceptualize the fundamental characteristics of the hot spot as a relatively planar, hydrophobic region surrounded by elements of protein specificity.

From active compounds discovered to disrupt protein–protein interactions, several conclusions can be drawn. With regard to peptides, virtually all structures possess tyrosine, tryptophan, and/or arginine.<sup>32,33</sup> For non-peptide molecules, most of them contain multiple aromatic rings connected by relatively rigid linkers that might be expected to prevent intramolecular hydrophobic collapse.<sup>33</sup> Based on these observations, we chose a planar, aromatic scaffold as an appropriate framework for our credit-card design. Using this scaffold, we envisioned that molecular diversity would be introduced in the form of pendant polar/hydrophobic functionalities. Therefore, the entire credit-card structure should provide the necessary combination of planarity,  $\pi$ -stacking interactions, hydrophilicity, and favorable entropy gain from hydrophobic effects to cover the necessary surface area and thus binding interactions with varying degrees of specificity. To satisfy these conditions, we considered diversity-oriented synthesis (DOS)<sup>48,50,63–65</sup> and the simple appending of building blocks to a common molecular scaffold.<sup>66,67</sup> We chose the latter, since it can be highly efficient and amenable to a variety of chemistries. While it may be argued that this approach provides limited access to three-dimensional space, our intent was to create a small library (less than 300) to examine quickly our proposed concept. Using multi-component coupling reactions like the Ugi reaction provides ease of access to inputs that allow the credit-card design with structural variability in the final library.

The importance of the transcription factor Myc in oncogenic transformation cannot be overstated. This protein contributes directly to a number of human cancers, and since its activity is dependent on binding to the

activation partner Max, inhibitors of the protein–protein interaction between Myc and Max are of therapeutic interest. The research groups of Boger and Prochownik have studied small molecule inhibitors of Myc–Max interactions.<sup>7,59</sup> Boger and co-workers have used an elegant solution-phase library approach to create and screen a library of 7000 members, while Prochownik screened a 10,000 member commercial library from Chembridge using a yeast two-hybrid assay. Both groups have found molecules that block Myc–Max interaction at the micromolar level. However, a direct comparison between the two approaches cannot be made as the assay systems are different. We note, however, that both groups found molecules that we define as having a credit-card structure, built on such frameworks as an isoindoline, 2-phenylchroman, and a carbazol.

Validation of our approach has been achieved by the use of credit-card compounds based on a naphthyl-scaffold. However, a myriad of other scaffolds fit within our conceptual framework. We prepared a small 285-membered library using the Ugi reaction with four points of chemical diversity. The components were readily obtained from commercial sources, and because the reactions were essentially one pot, work-up, isolation, and resynthesis of ‘hit’ compounds made the entire process efficient. Based on a FRET assay between cyan fluorescent protein-tagged Myc and yellow fluorescent protein-tagged Max, 40 compounds were selected from the library that reduced dimer association and produced a negative effect on the FRET signal at a concentration of 7.6  $\mu\text{M}$ . Four compounds advanced through the screening process when a more stringent and time-consuming EMSA was used to detect disruption of Myc–Max dimers. Using a synthetic Myc–Max dimer, the spectra of a denaturation mechanism for disruption of dimerization has been largely ruled out. Furthermore, a potential explanation for these compounds’ mode of action was proposed, namely, that they bind at the interface between the neighboring Myc and Max sequences, thus impeding their co-association without detriment to helicity.

The four compounds identified by EMSA (Fig. 2) are composed of aromatic and other hydrophobic motifs. Importantly, these compounds were potent enough to allow for  $\text{IC}_{50}$  values to be obtained from the EMSA (Fig. 3). Notably, NY2276 is one of the most potent small molecule inhibitors discovered to date for blocking Myc–Max dimerization in vitro.<sup>7,59</sup> Moreover, the compound was identified from a library more than 10-fold smaller than previously screened libraries. While conclusions about structure–activity are premature, we can make the following comments: (1) The *tert*-butyl ester functionality at the  $\text{R}^1$  position is found as a common motif shared by all four compounds; (2) The  $\text{R}^2$  and  $\text{R}^3$  positions utilized hydrophobic cyclohexyl, benzyl, *p*-methoxy-benzyl, and butyl functionalities; and (3) The  $\text{R}^4$  position invoked an aromatic functionality.

Two of the four selected compounds, NY2267 and NY2280, inhibited Myc-induced oncogenic transformation in cell culture. It is not clear why the EMSA-posi-

tive compounds NY2276 and NY2279 failed to affect Myc focus formation. As judged by their ability to interfere with transcriptional activation, these compounds are capable of entering cells. They may have off-target effects that cancel inhibition of transformation. The resistance of Src-induced transformation to the Myc inhibitors is unexpected, as Src transformation has been reported to depend on Myc.<sup>68,69</sup> However, the inhibitors cause only a partial reduction in Myc-dependent transcriptional regulation; the residual activity may be sufficient to support Src-induced transformation. Previously described inhibitors of Myc–Max dimerization also failed to affect Src. The activity of the Myc inhibitors in reporter assays measuring transcriptional activation is in concert with the results in EMSA and FRET. The negative control compounds, 6–8, had no effect on the transcriptional activities, which demonstrated that while the naphthyl-scaffold is a necessary component, it also requires structural points of diversity to be effective. The inhibition of Jun-dependent transcriptional activation requires further study, notably a determination of target molecules and binding sites. It is conceivable that the leucine zipper domains of Myc–Max and of Jun–Fos, Jun–Fra or Jun–ATF share some structural features that would make them common targets of the selected compounds. A possible interplay between Jun and Myc also remains to be investigated. More information on transcriptional effects of the compounds can also be obtained by measuring expression levels of known specific Myc, Jun or NF $\kappa$ B targets. Such studies are in progress.

Taken in total these observations suggest that the FRET, EMSA, and transcriptional reporter assays used in concert can identify small-molecule inhibitory compounds for disrupting protein–protein interactions which we have termed ‘credit-cards’, and several of these molecules form a subset of anti-oncogenic compounds. Future investigations will look at the generality of such an approach to other protein–protein interactions as well as refinement of the specificity of these interactions.

#### 4. Conclusion

The development of small molecules that can recognize protein surfaces and disrupt protein–protein interactions is of great interest, and such compounds have been difficult to identify. The most challenging aspect of this problem is the need to recognize relatively large and flat surface areas as opposed to well-organized clefts, as found, for example, in enzyme active sites. We have shown how a small well-designed library based on what we term ‘credit-card’ structures can effectively inhibit protein–protein interactions. The success of our approach is grounded upon a planar, aromatic scaffold that allowed the introduction of molecular diversity to achieve coverage and specificity at the interface domain. Validation of the design was accomplished by disrupting the Myc–Max interaction. Myc is a transcriptional regulator known to induce lymphoid tumors in animals and its deregulation is associated with numerous types of human cancers. The importance of this work is that it

identifies a small molecule strategy that can disrupt protein–protein interactions and provides a thought provoking hypothesis for previous/future reports of small molecule activity at protein–protein interfaces.

## 5. Experimental procedures

### 5.1. General procedure

The  $^1\text{H}$  NMR and  $^{13}\text{C}$  NMR spectra were recorded on a Bruker AMX-400 or Varian Inova-400 instrument. The following abbreviations were used to explain the multiplicities: s = singlet, d = doublet, t = triplet, q = quartet, m = multiplet, and br = broad. High-resolution mass spectra (HRMS) were recorded at The Scripps Research Institute on a VG ZAB-ZSE mass spectrometer using MALDI. All reactions were monitored by thin-layer chromatography (TLC) carried out on 0.25 mm E. Merck silica plates (60F-254), with fractions being visualized by UV light. Column chromatography was carried out with Mallinckrodt SilicAR 60 silica gel (40–60  $\mu\text{m}$ ). Reagent grade solvents for chromatography were obtained from Fisher Scientific. Reagents were purchased at the highest commercial quality and used without further purification. All reactions were carried out under an argon atmosphere, unless otherwise noted. Reported yields were determined after purification for a homogeneous material. Compounds **7** and **8** were purchased from Aldrich chemical company.

### 5.2. *tert*-Butyl 2-(naphthalene-2-yloxy)acetate (**6**)

To a solution of 2-naphthol (100 mg, 0.69 mmol) in DMF (5 mL) were added  $\text{K}_2\text{CO}_3$  (500 mg, 3.5 mmol) and *tert*-butyl bromoacetate (135 mg, 0.69 mmol). After stirring for 1 h at 60  $^\circ\text{C}$ , the mixture was cooled to room temperature and diluted with water. The product was extracted with diethyl ether twice. The combined organic layers were washed with water and then with brine. The organic layer was dried over  $\text{MgSO}_4$  and concentrated in vacuo. The residue was purified by silica gel column chromatography (20% EtOAc/hexane) to produce compound **6** (130 mg, 55% yield) as a light yellow oil.

$^1\text{H}$  NMR ( $\text{CDCl}_3$ , 400 MHz):  $\delta$  1.51 (s, 9H), 4.64 (s, 2H), 7.01 (s, 1H), 7.25 (t,  $J = 8.84$  Hz, 1H), 7.36 (t,  $J = 7.45$  Hz, 1H), 7.45 (t,  $J = 7.24$  Hz, 1H), 7.71 (d,  $J = 8.16$ , 1H), 7.77 (m, 2H).

$^{13}\text{C}$  NMR ( $\text{CDCl}_3$ , 100 MHz):  $\delta$  28.03, 65.75, 82.40, 106.99, 118.63, 123.93, 126.41, 126.79, 127.63, 129.29, 129.61, 134.24, 155.80, 167.91.

MALDI-FTMS Calcd for  $\text{C}_{16}\text{H}_{18}\text{O}_3\text{Na}$  ( $\text{M}^+ + \text{Na}$ ): 281.1148. Found: 281.1146.

### 5.3. (6-Formyl-naphthalen-2-yloxy)-acetic acid *tert*-butyl ester

To a solution of 6-hydroxy-naphthalene-2-carbaldehyde (1.72 g, 10 mmol) in DMF (30 mL) were added

$\text{K}_2\text{CO}_3$  (6.9 g, 50 mmol) and *tert*-butyl bromoacetate (2.34 g, 12 mmol). After stirring for 1 h at 60  $^\circ\text{C}$ , the mixture was cooled to room temperature and diluted with water. The product was extracted with diethyl ether twice. The combined organic layers were washed with water and then with brine. The organic layer was dried over  $\text{MgSO}_4$  and concentrated in vacuo, the residue purified by silica gel column chromatography (20% EtOAc/hexane) to produce (6-formyl-naphthalen-2-yloxy)-acetic acid *tert*-butyl ester (2.63 g, 92% yield) as white crystals. This material was utilized as compound **3** for the preparation of NY2267, NY2276, NY2279, and NY2280.

$^1\text{H}$  NMR ( $\text{CDCl}_3$ , 400 MHz):  $\delta$  1.51 (s, 9H), 4.67 (s, 2H), 7.10 (d,  $J = 2.4$  Hz, 1H), 7.32 (dd,  $J = 2.4$  Hz, 11.2 Hz, 1H), 7.78 (d,  $J = 8.4$  Hz, 1H), 7.93 (d,  $J = 8.4$  Hz, 1H), 7.93 (d,  $J = 11.2$  Hz, 1H) 8.21 (s, 1H), 10.1 (d,  $J = 0.4$  Hz, 1H).

$^{13}\text{C}$  NMR ( $\text{CDCl}_3$ , 100 MHz):  $\delta$  28.0, 65.6, 82.7, 107.2, 119.8, 123.6, 127.8, 131.3, 137.9, 158.4, 167.4, 192.0.

MALDI-FTMS Calcd for  $\text{C}_{17}\text{H}_{19}\text{O}_4$  ( $\text{M}^+ + \text{H}$ ): 287.1278. Found: 287.1283.

### 5.4. General procedure for the preparation of Ugi 4-component reaction library

To a solution of the naphthal derivative **3** (0.2 mmol, 1.0 equiv) in MeOH were added acid (0.4 mmol, 2.0 equiv), amine 0.4 mmol, (2.0 equiv), and isocyanide (0.4 mmol, 2.0 equiv). After stirring for 24 h at reflux, the mixture was cooled to room temperature and concentrated in vacuo. The residue was purified by a short silica gel column packed in a 5 mL Teflon syringe with 10–50% EtOAc/hexane gradient to afford the product. The products were analyzed by  $^1\text{H}$  NMR and HRMS.

### 5.5. (6-{Cyclohexylcarbonyl-[(4-methoxy-benzyl)-(pyridine-2-carbonyl)-amino]-methyl}-naphthalen-2-yloxy)-acetic acid *tert*-butyl ester (NY2267)

NY2267 was produced as a colorless oil (59.5 mg, 47% yield).

$^1\text{H}$  NMR ( $\text{DMSO}-d_6$ , 400 MHz)  $\delta$  0.85–1.25 (m, 5H), 1.43 (s, 9H), 1.48–1.75 (m, 5H), 3.54 (s, 2H), 3.58 (s, 3H), 4.30–4.52 (m, 1H), 4.76 (s, 2H), 5.83 (s, 1H), 6.32 (s, 1H), 6.43 (d,  $J = 7.77$  Hz, 1H), 6.51 (d,  $J = 8.09$  Hz, 1H), 6.62 (d,  $J = 7.75$  Hz, 1H), 6.808 (d,  $J = 7.9$  Hz, 1H), 7.16–8.67 (m, 10H).

$^{13}\text{C}$  NMR ( $\text{DMSO}-d_6$ , 100 MHz)  $\delta$  24.36, 25.08, 27.62, 32.02, 54.77, 55.03, 60.85, 64.15, 64.99, 81.37, 106.86, 112.70, 112.80, 118.52, 122.84, 124.57, 126.60, 127.38, 127.77, 128.12, 129.52, 130.45, 130.57, 131.26, 131.57, 133.36, 136.79, 137.41, 154.28, 155.79, 157.37, 167.60, 167.96, 169.50.

MALDI-FTMS Calcd for  $\text{C}_{38}\text{H}_{44}\text{N}_3\text{O}_6$  ( $\text{M}^+ + \text{H}$ ): 638.3224. Found: 638.3234.

**5.6. [6-(Cyclohexylcarbamoyl-[(4-methoxy-benzyl)-[2-(4-methoxy-phenyl)-acetyl]-amino]-methyl)-naphthalen-2-yloxy]-acetic acid *tert*-butyl ester (NY2276)**

NY2276 was produced as a colorless oil (132 mg, 99%).

<sup>1</sup>H NMR (CDCl<sub>3</sub>, 400 MHz): δ 0.94–1.40 (m, 5H), 1.49 (s, 9H), 1.50–1.96 (m, 5H), 3.54–3.67 (m, 2H), 3.70 (s, 3H), 3.74–3.82 (m, 1H), 3.76 (s, 3H), 4.47 (d, *J* = 17.2 Hz, 1H), 4.605 (s, 2H), 4.68 (d, *J* = 17.2 Hz, 1H), 5.82–5.90 (m, 1H), 5.97 (s, 1H), 6.67 (d, *J* = 8.4 Hz, 2H), 6.81 (d, *J* = 8.0 Hz, 2H), 6.93 (d, *J* = 8.4 Hz, 2H), 6.99 (br s, 1H), 7.09 (d, *J* = 8.0 Hz, 2H), 7.20 (dd, *J* = 1.6 Hz, 9.2 Hz, 1H), δ 37 (d, *J* = 8.8 Hz, 1H), 7.57 (d, *J* = 8.8 Hz, 1H), 7.63 (d, *J* = 9.2 Hz, 1H), 7.70 (s, 1H).

<sup>13</sup>C NMR (CDCl<sub>3</sub>, 100 MHz) δ 24.6, 24.7, 25.4, 27.9, 32.6, 40.4, 48.4, 49.7, 55.1, 63.1, 65.6, 77.2, 82, 106.7, 113.7, 113.9, 126.7, 127.2, 127.4, 127.5, 128.78, 128.82, 129.3, 129.6, 129.7, 129.9, 130.7, 131.0, 133.8, 156.3, 158.4, 158.5, 167.7, 168.5, 173.1.

MALDI-FTMS Calcd for C<sub>41</sub>H<sub>48</sub>N<sub>2</sub>O<sub>7</sub>Na (M<sup>+</sup>+Na): 703.3354. Found: 703.3380.

**5.7. [6-(Benzylcarbamoyl-[(4-methoxy-benzyl)-[2-(4-methoxy-phenyl)-acetyl]-amino]-methyl)-naphthalen-2-yloxy]-acetic acid *tert*-butyl ester (NY2279)**

NY2279 was produced as a colorless oil (133 mg, 99%).

<sup>1</sup>H NMR (CDCl<sub>3</sub>, 400 MHz): δ 1.50 (s, 9H), 3.59–3.65 (m, 1H), 3.70 (s, 3H), 3.75 (s, 3H), 4.34–4.46 (m, 2H), 4.51 (d, *J* = 17.2 Hz, 1H), 4.70 (d, *J* = 17.2 Hz, 1H), 6.07 (s, 1H), 6.55 (m, 1H), 6.66 (d, *J* = 8.4 Hz, 2H), 6.79 (d, *J* = 8.4 Hz, 2H), 6.91 (d, *J* = 8.4 Hz, 2H), 6.99 (br s, 1H), 7.07 (d, *J* = 8.4 Hz, 2H), 7.15–7.32 (m, 6H), 7.37 (d, *J* = 9.2 Hz), 7.56 (d, *J* = 8.8 Hz, 1H), 7.59 (d, *J* = 9.2 Hz, 1H), 7.69 (s, 1H).

<sup>13</sup>C NMR (CDCl<sub>3</sub>, 100 MHz): δ 28.3, 40.6, 43.8, 50.1, 55.4, 63.5, 66.0, 82.7, 107.0, 114.1, 114.2, 114.3, 126.9, 127.48, 127.55, 127.7, 127.9, 128.8, 129.1, 130.0, 130.2, 130.6, 130.7, 134.2, 138.3, 156.7, 158.8, 158.9, 168.0, 170.0, 173.6.

MALDI-FTMS Calcd for C<sub>42</sub>H<sub>44</sub>N<sub>2</sub>O<sub>7</sub>Na (M<sup>+</sup>+Na): 711.3041. Found: 711.3016.

**5.8. [6-(Benzylcarbamoyl-[(butyl)-[2-(4-methoxy-phenyl)-acetyl]-amino]-methyl)-naphthalen-2-yloxy]-acetic acid *tert*-butyl ester (NY2280)**

NY2280 was produced as a colorless oil (109 mg, 87%).

<sup>1</sup>H NMR (CDCl<sub>3</sub>, 400 MHz): δ 0.66 (t, *J* = 7.2 Hz, 2H), 0.90–1.10 (m, 2H), 1.34–1.56 (m, 3H), 1.50 (s, 3H), 3.30–3.37 (m, 2H), 3.50–3.80 (m, 2H), 3.78 (s, 3H), 4.42 (dd, *J* = 5.6 Hz, 15.2 Hz, 1H), 4.48 (dd, *J* = 5.6 Hz, 15.2 Hz, 1H), 4.63 (s, 2H), 6.00 (s, 1H), 6.55 (t, *J* = 5.6 Hz, 1H), 6.76–6.86 (m, 2H), 6.94–7.34 (m, 10H), 7.40 (dd,

*J* = 2.0 Hz, 8.8 Hz, 1H), 7.66 (d, *J* = 8.8 Hz, 1H), 7.67 (d, *J* = 8.8 Hz, 1H).

<sup>13</sup>C NMR (CDCl<sub>3</sub>, 100 MHz): δ 13.4, 19.9, 28.0, 31.89, 40.0, 43.6, 47.2, 55.2, 62.9, 65.7, 82.5, 106.8, 114.0, 119.1, 126.9, 127.3, 127.5, 127.6, 128.3, 128.4, 128.5, 129.0, 129.8, 129.9, 130.7, 133.9, 138.0, 156.4, 158.4, 167.8, 169.9, 172.4.

MALDI-FTMS Calcd for C<sub>42</sub>H<sub>44</sub>N<sub>2</sub>Na (M<sup>+</sup>+Na): 711.3041. Found: 711.3016.

**5.9. Synthetic Myc–S–Max dimer**

N-terminal-bromoacetyl-Myc (BrAc-Myc) and N-terminal-3-mercaptopropionyl-Max (Mpa-Max) peptides were prepared by stepwise SPPS on a 1.0 mmol scale using in situ neutralization protocols for Boc chemistry custom-written for a CSBio 136 automated peptide synthesizer (available by request from author). All Boc amino acids and HBTU were obtained from Senn Chemicals (Dielsdorf, Switzerland). *p*-Methylbenzhydrylamine (MBHA) resin was prepared by Advanced Chemtech as a custom synthesis at a loading of 0.64 mmol NH<sub>2</sub>/g (100–200 mesh). Side chain protections were as follows: Ser/Thr (Bzl), Asp/Glu (OcHex), His (Bom and Dnp, vide infra), Tyr (2-BrZ), Lys (2-CIZ), Arg (Tos), and Asn (Xan); all other amino acids were incorporated without side chain protection. Trifluoroacetic acid (Biograde) was from Halocarbon (River Edge, NJ), *N,N*-dimethylformamide (BioAnalyzed) was from J. T. Baker (St. Louis, MO) and EMD (Gibbstown, NJ), *N,N*-diisopropylethylamine (Atofina EDIPA) was from Aldrich (Milwaukee, WI), and anhydrous hydrogen fluoride (CP grade) was from Matheson Gas (Cucamonga, CA). HF cleavage was performed in a Type II vacuum-driven HF apparatus from Peptide Institute (Minoh, Osaka, Japan). All other reagents, solvents, and chemicals were of the highest purity commercially available and used as received. RP-HPLC was performed employing binary gradients of solvents A and B, where A is 0.1% TFA in water and B is 0.09% TFA in acetonitrile. Analytical RP-HPLC was performed using a Vydac 218TP5415 column at a flow rate of 1 mL/min, with detection at 214 nm during a linear gradient of 10–50%B over 30 min. Preparative RP-HPLC was performed using a Vydac 218TP101522 column at a flow rate of 10 mL/min, with detection at 230 nm during a linear gradient of 25–45% B over 30 min. In all cases, fractions were analyzed off-line using an ABI/Sciex 150EX single quadrupole mass spectrometer and judged for purity after a consistent summing of 50 scans in multi-channel analysis (MCA) mode. For preparative purification purposes, fractions that contained no consistent charged species which accounted for more than 10% of the total ion intensity were designated 'pure' and pooled; the homogeneity of this pool was verified by analytical RP-HPLC and was >95%. All purification and manipulation steps were performed at ambient temperature unless otherwise indicated.

For BrAc-Myc, the N-terminus was bromoacetylated using 5 equiv bromoacetic anhydride. This reagent was prepared immediately prior to use by reacting 10 mmol bromoacetic acid and 5 mmol *N,N'*-diisopropylcarbodiimide in 10 mL  $\text{CH}_2\text{Cl}_2$ ; after 10 min pre-activation, this gelatinous mixture was diluted with one volume of DMF and added to the pre-neutralized peptide-resin. Ninhydrin analysis indicated that this coupling was complete in 20 min, after which the peptide-resin was dried in vacuo overnight and then treated with HF (15 mL/g peptide-resin) containing 2.5 wt % each of *p*-cresol and resorcinol for 1 h at 0 °C. It should be noted that His(Bom) was used for this synthesis because on-resin thiolytic deprotection of His(Dnp) would have destroyed the bromoacetyl moiety. After evaporation of HF, the peptide was extracted from the resin with TFA; this filtrate was then concentrated by centrifugal evaporation and the peptide recovered and washed using three successive triturations with 10 volumes of diethyl ether (chilled to  $-20^\circ\text{C}$ ). The crude peptide was then solubilized in aqueous acetonitrile (containing 0.1% TFA) and lyophilized for purification. For Mpa-Max, *S*-trityl-mercaptopropionic acid (3 equiv) was coupled to the N-terminus using BOP (4 equiv) with excess DIEA in DMF. Ninhydrin analysis indicated that this coupling was complete in 30 min, after which the His(Dnp) protection was removed by three successive 10 min batchwise treatments with  $\beta$ -mercaptoethanol:DIEA:DMF (2:1:7 by volume). The N-terminal trityl thioether was then deprotected by three successive 2 min batchwise treatments with TFA containing 2 vol % each of TIS and 3,6-dioxa-1,8-octanedithiol. The peptide-resin was then dried in vacuo overnight; HF cleavage and isolation of the peptide were performed as in the case of BrAc-Myc, with the exception that 5 wt % *p*-cresol was used as the sole scavenger. The Myc-S-Max dimer was prepared by a chemoselective thioether ligation strategy. Forty milligrams of each peptide was dissolved in 4 mL  $\text{N}_2$ -purged 0.5 M triethanolamine containing 6 M GuHCl, buffered at pH 8.0. After 16 h, RP-HPLC indicated that the reaction was complete; this material was then purified by preparative RP-HPLC and used in CD experiments. MW 7477.5, ESI-MS *M/Z* ions (theory):  $\text{M}^{4+}$  1870.4,  $\text{M}^{5+}$  1496.5,  $\text{M}^{6+}$  1247.3,  $\text{M}^{7+}$  1069.2,  $\text{M}^{8+}$  935.7,  $\text{M}^{9+}$  831.8; (observed):  $\text{M}^{4+}$  1870.6,  $\text{M}^{5+}$  1496.7,  $\text{M}^{6+}$  1247.1,  $\text{M}^{7+}$  1069.6,  $\text{M}^{8+}$  936.0,  $\text{M}^{9+}$  832.2.

### 5.10. CD experiments

Far-UV circular dichroism spectra were obtained on an Aviv Model 202 instrument with a 1 cm path length fused silica cell at 25 °C. Purified Myc-S-Max was reconstituted at 100  $\mu\text{M}$  and diluted 10-fold into four separate solutions of selected library members at 25  $\mu\text{M}$  in phosphate-buffered saline, pH 7.4, containing 5 vol % DMSO. Data are corrected for blank absorbance of each compound and are the average of three scans.

### 5.11. Recombinant proteins

The fusion constructs of the basic helix-loop-helix leucine zipper (bHLHZip) domains of the Myc or the

Max protein to cyan fluorescent protein (CFP) or yellow fluorescent protein (YFP) were described previously (Berg, 2003). They were expressed by the histidine-tag vector pET28a (Novagen) to produce MycCFP and MaxYFP. A fusion construct of the Myc bHLHZip domain to green fluorescent protein (GFP) was produced following the same protocols and was used in the electrophoretic mobility shift assays. The bHLHZip domain (amino acids 13–93) of rat Max with C-terminal AU1 tag was also cloned into pET28a. Proteins were expressed in *Escherichia coli* strain BL21(DE3), purified by affinity chromatography on nickel columns, and dialyzed against buffer containing 200 mM Hepes (pH 7.0), 500 mM KCl, 30 mM  $\text{MgCl}_2$ , 2 mM DTT, and 10 mM EDTA (referred to as 1 $\times$  Max buffer).

### 5.12. Fluorescence resonance energy transfer

The bHLHZip domains of Myc and of Max were fused to the N termini of CFP (MycCFP) and YFP (MaxYFP), respectively. The fusions were expressed in *E. coli*, purified, and allowed to dimerize, followed by excitation of CFP at wavelength 433 nm. Dimerization generated a FRET spectrum characterized by a strong emission signal of YFP at 525 nm. In control experiments, the ratios of fluorescence intensities at 525 nm over 475 nm were 1.7 at complete dimerization of MycCFP with MaxYFP and 0.4 for the monomeric state of Myc CFP. One hundred percent inhibition of MycCFP/MaxYFP dimerization was achieved by addition of 100 $\times$  molar excess of the bHLHZip domain of Max, functioning as a competitive inhibitor of Myc-Max dimerization, resulting in a 525/475 nm ratio of slightly more than 0.4. To screen for potential inhibitors of dimerization, compounds were added to a final concentration of 7.6  $\mu\text{M}$  and 7.6% DMSO, and the mixture of each compound with MycCFP and MaxYFP (at 80 nM monomer concentration) was incubated in 1 $\times$  Max buffer for 1 h at room temperature. After excitation of CFP at 433 nm, both the CFP fluorescence at 475 nm and the YFP fluorescence at 525 nm were measured in a 96-well fluorescence plate reader (Molecular Devices). Dimerization generates a FRET signal that causes the emission of CFP at 475 nm to decrease, while enhancing the emission of YFP at 525 nm. Compounds that dissociate MycCFP/MaxYFP dimers increase the emission of CFP and decrease the emission of YFP. Presumptive inhibitors were retested in single-cuvettes on a Perkin-Elmer LS 50B to confirm the fluorescence data.

### 5.13. Electrophoretic mobility shift assay

MycGFP and Max were mixed and incubated with screening compounds for 1 h at room temperature. The candidate compounds were tested at the concentrations indicated in the figure legends. All test mixtures contained 10% DMSO. A double-stranded DNA oligonucleotide with the consensus binding site of Myc-Max dimers (5'AGTTGACCACGTGGTCTGGG 3') was then added. The DNA-protein interaction was allowed to proceed for 30 min. As control, a mutated probe was used (5'AGTTGACTACGTAGTCTGGG3'). Final concentrations were: 50 nM MycGFP, 27.5 nM Max, 200 mM

Hepes (pH 7.0), 500 mM KCl, 30 mM MgCl<sub>2</sub>, 2 mM DTT, 10 mM EDTA, 5% glycerol, 40 ng/μL salmon testis DNA (Sigma), and 60 pg/μL <sup>32</sup>P-labeled oligonucleotide probe. Protein–DNA complexes were resolved on 4% acrylamide gels and detected by autoradiography. The concentration of compounds causing 50% inhibition of Myc–Max dimerization was determined by densitometry of the shifted band. Densitometry was performed by using the NIH Image 1.63 software program.

#### 5.14. Luciferase assays

HEK293 cells were seeded at  $5 \times 10^4$  in 24-well plates and transfected on the next day with PolyFect (Qiagen) and appropriate combinations of reporter and expression vectors in the following amounts: 100 ng Myc-response luciferase reporter vector pGLM4, 2 ng Renilla control vector pRLCMV, and either 300 ng pcDNA3 or 300 ng pCMV3HuMyc expressing the human Myc protein JEG-3 cells were transfected with PolyFect and the following vectors: 100 ng Jun-dependent luciferase reporter vector pRBGB + c-Jun-site, 2 ng Renilla control vector pRLCMV, and either 300 ng c-Jun expression vector pEF2hyg-cJun or control vector pEF2hyg. Luciferase activity was assayed 48 h after transfection using the dual-luciferase reporter assay system (Promega). Where noted, compound was added to cells 24 h after transfection. All assays were normalized for transfection efficiency by using a co-transfected-Renilla expression vector pRLCMV vector. Assays were performed in triplicate.

#### 5.15. Focus assays

CEF were seeded at  $1.5 \times 10^5$  cells per 12-well tissue culture plate in HAM's F10 containing 10% FBS. One day after seeding, the cells were infected with 10-fold serial dilutions of oncogenic retroviruses. These viruses were: (i) the RCAS viral vector expressing chicken cellular Myc, (ii) the Prague strain of Rous sarcoma virus, coding for the Src oncoprotein, and (iii) the avian sarcoma virus 17, expressing the oncoprotein v-Jun. The cultures were then overlaid with nutrient agarose consisting of 57.5% (v/v) of media (75% F10 2x, 5% FBS, 2% chicken serum, 15% tryptose–phosphate broth, 1.5% of L-glutamine/penicillin/streptomycin solution, and screening compounds in DMSO, final concentration of DMSO: 0.3%) and 42.5% (v/v) of 1.5% Sea Plaque Agarose. After three weeks, cultures were stained with 2% crystal violet.

#### Acknowledgments

This work was supported by the Skaggs Institute for Chemical Biology and by grants from the National Cancer Institute and the California Breast Cancer Research Program.

#### References and notes

- Ho, Y.; Gruhler, A.; Heilbut, A.; Bader, G. D.; Moore, L.; Adams, S. L.; Millar, A.; Taylor, P.; Bennett, K.; Boutillier, K.; Yang, L. Y.; Wolting, C.; Donaldson, I.; Schandorff, S.; Shewnarane, J.; Vo, M.; Taggart, J.; Goudreault, M.; Muskat, B.; Alfarano, C.; Dewar, D.; Lin, Z.; Michalickova, K.; Willems, A. R.; Sassi, H.; Nielsen, P. A.; Rasmussen, K. J.; Andersen, J. R.; Johansen, L. E.; Hansen, L. H.; Jespersen, H.; Podtelejnikov, A.; Nielsen, E.; Crawford, J.; Poulsen, V.; Sorensen, B. D.; Matthiesen, J.; Hendrickson, R. C.; Gleeson, F.; Pawson, T.; Moran, M. F.; Durocher, D.; Mann, M.; Hogue, C. W. V.; Figeys, D.; Tyers, M. *Nature* **2002**, *415*, 180–183.
- Gavin, A. C.; Bosche, M.; Krause, R.; Grandi, P.; Marzioch, M.; Bauer, A.; Schultz, J.; Rick, J. M.; Michon, A. M.; Cruciat, C. M.; Remor, M.; Hofert, C.; Schelder, M.; Brajenovic, M.; Ruffner, H.; Merino, A.; Klein, K.; Hudak, M.; Dickson, D.; Rudi, T.; Gnau, V.; Bauch, A.; Bastuck, S.; Huhse, B.; Leutwein, C.; Heurtier, M. A.; Copley, R. R.; Edelman, A.; Querfurth, E.; Rybin, V.; Drewes, G.; Raida, M.; Bouwmeester, T.; Bork, P.; Seraphin, B.; Kuster, B.; Neubauer, G.; Superti-Furga, G. *Nature* **2002**, *415*, 141–147.
- Berg, T. *Angew. Chem., Int. Ed.* **2003**, *42*, 2462–2481.
- Veselovsky, A. V.; Ivanov, Y. D.; Ivanov, A. S.; Archakov, A. I.; Lewi, P.; Janssen, P. *J. Mol. Recognit.* **2002**, *15*, 405–422.
- Arkin, M. R.; Wells, J. A. *Nat. Rev. Drug Disc.* **2004**, *3*, 301–317.
- Berg, T. *Chembiochem* **2004**, *5*, 1051–1053.
- Berg, T.; Cohen, S. B.; Desharnais, J.; Sonderegger, C.; Maslyar, D. J.; Goldberg, J.; Boger, D. L.; Vogt, P. K. *Proc. Natl. Acad. Sci. U.S.A.* **2002**, *99*, 3830–3835.
- Arkin, M. R.; Randal, M.; DeLano, W. L.; Hyde, J.; Luong, T. N.; Oslob, J. D.; Raphael, D. R.; Taylor, L.; Wang, J.; McDowell, R. S.; Wells, J. A.; Braisted, A. C. *Proc. Natl. Acad. Sci. U.S.A.* **2003**, *100*, 1603–1608.
- Carlson, H. A. *Curr. Opin. Chem. Biol.* **2002**, *6*, 447–452.
- Greenbaum, D. C.; Arnold, W. D.; Lu, F.; Hayrapetian, L.; Baruch, A.; Krumrine, J.; Toba, S.; Chehade, K.; Bromme, D.; Kuntz, I. D.; Bogyo, M. *Chem. Biol.* **2002**, *9*, 1085–1094.
- Cheng, S.; Tarby, C. M.; Comer, D. D.; Williams, J. P.; Caporale, L. H.; Myers, P. L.; Boger, D. L. *Bioorg. Med. Chem.* **1996**, *4*, 727–737.
- Terrett, N. K.; Gardner, M.; Gordon, D. W.; Kobylecki, R. J.; Steele, J. *Tetrahedron* **1995**, *51*, 8135–8173.
- Janda, K. D. *Proc. Natl. Acad. Sci. U.S.A.* **1994**, *91*, 10779–10785.
- Gallop, M. A.; Barrett, R. W.; Dower, W. J.; Fodor, S. P. A.; Gordon, E. M. *J. Med. Chem.* **1994**, *37*, 1233–1251.
- Pavia, M. R.; Sawyer, T. K.; Moos, W. H. *Bioorg. Med. Chem. Lett.* **1993**, *3*, 387–396.
- Duesberg, P. H.; Vogt, P. K. *Proc. Natl. Acad. Sci. U.S.A.* **1979**, *76*, 1633–1637.
- Duesberg, P. H.; Bister, K.; Vogt, P. K. *Proc. Natl. Acad. Sci. U.S.A.* **1977**, *74*, 4320–4324.
- Amati, B.; Littlewood, T. D.; Evan, G. I.; Land, H. *EMBO J.* **1993**, *12*, 5083–5087.
- Atchley, W. R.; Fitch, W. M. *Proc. Natl. Acad. Sci. U.S.A.* **1997**, *94*, 5172–5176.
- Dang, C. V.; Lewis, B. C. *J. Biomed. Sci.* **1997**, *4*, 269–278.
- Dang, C. V.; McGuire, M.; Buckmire, M.; Lee, W. M. F. *Nature* **1989**, *337*, 664–666.
- Davis, L. J.; Halazonetis, T. D. *Oncogene* **1993**, *8*, 125–132.
- Fisher, D. E.; Parent, L. A.; Sharp, P. A. *Proc. Natl. Acad. Sci. U.S.A.* **1992**, *89*, 11779–11783.
- Dang, C. V.; Resar, L. M. S.; Emison, E.; Kim, S.; Li, Q.; Prescott, J. E.; Wonsey, D.; Zeller, K. *Exp. Cell Res.* **1999**, *253*, 63–77.

25. Morrish, F.; Giedt, C.; Hockenbery, D. *Genes Dev.* **2003**, *17*, 240–255.
26. Nesbit, C. E.; Tersak, J. M.; Grove, L. E.; Drzal, A.; Choi, H.; Prochownik, E. V. *Oncogene* **2000**, *19*, 3200–3212.
27. Amati, B.; Brooks, M. W.; Levy, N.; Littlewood, T. D.; Evan, G. I.; Land, H. *Cell* **1993**, *72*, 233–245.
28. Blackwood, E. M.; Eisenman, R. N. *Science* **1991**, *251*, 1211–1217.
29. Blackwood, E. M.; Luscher, B.; Eisenman, R. N. *Genes Dev.* **1992**, *6*, 71–80.
30. Blackwood, E. M.; Luscher, B.; Kretzner, L.; Eisenman, R. N. *Cold Spring Harb. Symp. Quant. Biol.* **1991**, *56*, 109–117.
31. Lo Conte, L.; Chothia, C.; Janin, J. *J. Mol. Biol.* **1999**, *285*, 2177–2198.
32. Stites, W. E. *Chem. Rev.* **1997**, *97*, 1233–1250.
33. Jones, S.; Thornton, J. M. *Proc. Natl. Acad. Sci. U.S.A.* **1996**, *93*, 13–20.
34. Lawrence, M. C.; Colman, P. M. *J. Mol. Biol.* **1993**, *234*, 946–950.
35. Hu, Z. J.; Ma, B. Y.; Wolfson, H.; Nussinov, R. *Proteins—Struct. Funct. Genet.* **2000**, *39*, 331–342.
36. Bogan, A. A.; Thorn, K. S. *J. Mol. Biol.* **1998**, *280*, 1–9.
37. DeLano, W. L. *Curr. Opin. Struct. Biol.* **2002**, *12*, 14–20.
38. Ma, B. Y.; Wolfson, H. J.; Nussinov, R. *Curr. Opin. Struct. Biol.* **2001**, *11*, 364–369.
39. Domling, A.; Ugi, I. *Angew. Chem., Int. Ed.* **2000**, *39*, 3169–3210.
40. Ugi, I. *Angew. Chem., Int. Ed. Engl.* **1962**, *74*, 9.
41. Ugi, I. *Angew. Chem., Int. Ed. Engl.* **1959**, *71*, 386.
42. Ugi, I.; Meyr, R. *Angew. Chem., Int. Ed. Engl.* **1958**, *70*, 702–703.
43. Posner, G. H. *Chem. Rev.* **1986**, *86*, 831–844.
44. Kolasa, T.; Gunn, D. E.; Bhatia, P.; Basha, A.; Craig, R. A.; Stewart, A. O.; Bouska, J. B.; Harris, R. R.; Hulkower, K. I.; Malo, P. E.; Bell, R. L.; Carter, G. W.; Brooks, C. D. W. *J. Med. Chem.* **2000**, *43*, 3322–3334.
45. Boger, D. L.; Desharnais, J.; Capps, K. *Angew. Chem., Int. Ed.* **2003**, *42*, 4138–4176.
46. Lavigne, P.; Kondejewski, L. H.; Houston, M. E.; Sonnichsen, F. D.; Lix, B.; Sykes, B. D.; Hodges, R. S.; Kay, C. M. *J. Mol. Biol.* **1995**, *254*, 505–520.
47. Lavigne, P.; Crump, M. P.; Gagne, S. M.; Hodges, R. S.; Kay, C. M.; Sykes, B. D. *J. Mol. Biol.* **1998**, *281*, 165–181.
48. Burke, M. D.; Schreiber, S. L. *Angew. Chem., Int. Ed.* **2004**, *43*, 46–58.
49. Edwards, P. J. *Comb. Chem. High Throughput Screening* **2003**, *6*, 11–27.
50. Spring, D. R.; Krishnan, S.; Blackwell, H. E.; Schreiber, S. L. *J. Am. Chem. Soc.* **2002**, *124*, 1354–1363.
51. Bhattacharyya, S. *Curr. Med. Chem.* **2001**, *8*, 1383–1404.
52. Sternson, S. M.; Wong, J. C.; Grozinger, C. M.; Schreiber, S. L. *Org. Lett.* **2001**, *3*, 4239–4242.
53. Ozbal, C. C.; LaMarr, W. A.; Linton, J. R.; Green, D. F.; Katz, A.; Morrison, T. B.; Brennan, C. J. H. *Assay Drug Dev. Technol.* **2004**, *2*, 373–381.
54. Cheon, H. G.; Lee, C. M.; Kim, B. T.; Hwang, K. J. *Bioorg. Med. Chem. Lett.* **2004**, *14*, 2661–2664.
55. Parniak, M. A.; Min, K. L.; Budihis, S. R.; Le Grice, S. F. J.; Beutler, J. A. *Anal. Biochem.* **2003**, *322*, 33–39.
56. Koehler, R. T.; Villar, H. O. *J. Comput. Chem.* **2000**, *21*, 1145–1152.
57. Li, L.; Thomas, R. M.; Suzuki, H.; De Brabander, J. K.; Wang, X. D.; Harran, P. G. *Science* **2004**, *305*, 1471–1474.
58. Muller, O.; Gourzoulidou, E.; Carpintero, M.; Karaguni, I. M.; Langerak, A.; Herrmann, C.; Moroy, T.; Klein-Hitpass, L.; Waldmann, H. *Angew. Chem., Int. Ed.* **2004**, *43*, 450–454.
59. Yin, X. Y.; Giap, C.; Lazo, J. S.; Prochownik, E. V. *Oncogene* **2003**, *22*, 6151–6159.
60. Cochran, A. G. *Chem. Biol.* **2000**, *7*, R85–R94.
61. Ferrer, M.; Kapoor, T. M.; Strassmaier, T.; Weissenhorn, W.; Skehel, J. J.; Oprian, D.; Schreiber, S. L.; Wiley, D. C.; Harrison, S. C. *Nat. Struct. Biol.* **1999**, *6*, 953–960.
62. Pearce, K. H.; Ultsch, M. H.; Kelley, R. F.; deVos, A. M.; Wells, J. A. *Biochemistry* **1996**, *35*, 10300–10307.
63. Taylor, S. J.; Taylor, A. M.; Schreiber, S. L. *Angew. Chem., Int. Ed.* **2004**, *43*, 1681–1685.
64. Schreiber, S. L. *Abstr. Papers Am. Chem. Soc.* **2003**, *226*, U238.
65. Schreiber, S. L. *Abstr. Papers Am. Chem. Soc.* **2002**, *224*, U177.
66. Dewitt, S. H.; Kiely, J. S.; Stankovic, C. J.; Schroeder, M. C.; Cody, D. M. R.; Pavia, M. R. *Proc. Natl. Acad. Sci. U.S.A.* **1993**, *90*, 6909–6913.
67. Bunin, B. A.; Ellman, J. A. *J. Am. Chem. Soc.* **1992**, *114*, 10997–10998.
68. Bowman, T.; Broome, M. A.; Sinibaldi, D.; Wharton, W.; Pledger, W. J.; Sedivy, J. M.; Irby, R.; Yeatman, T.; Courtneidge, S. A.; Jove, R. *Proc. Natl. Acad. Sci. U.S.A.* **2001**, *98*, 7319–7324.
69. Johnson, D.; Agochiya, M.; Samejima, K.; Earnshaw, W.; Frame, M.; Wyke, J. *Cell Death Differ.* **2000**, *7*, 685–696.